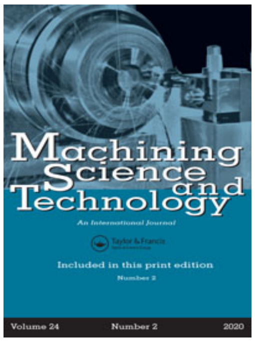

Machining Science and Technology
An International Journal

ISSN: 1091-0344 (Print) 1532-2483 (Online) Journal homepage: https://www.tandfonline.com/loi/lmst20

Fabrication of micro-end mill tool by EDM and its performance evaluation

Ganesh Malayath, Ajay M. Sidpara & Sankha Deb

To cite this article: Ganesh Malayath, Ajay M. Sidpara & Sankha Deb (2020) Fabrication of micro-end mill tool by EDM and its performance evaluation, Machining Science and Technology, 24:2, 169-194, DOI: 10.1080/10910344.2019.1636269

To link to this article: https://doi.org/10.1080/10910344.2019.1636269

MACHINING SCIENCE AND TECHNOLOGY
2020, VOL. 24, NO. 2, 169–194
https://doi.org/10.1080/10910344.2019.1636269

Fabrication of micro-end mill tool by EDM and its performance evaluation

Ganesh Malayath, Ajay M. Sidpara, and Sankha Deb

Mechanical Engineering Department, Indian Institute of Technology Kharagpur, Kharagpur, India

ABSTRACT

Micro-milling is a fast, cheap and controlled process compared to other micro-fabrication processes such as lithography, laser/electron/ion beam machining, etc. However, scarcity of cutting tools of very small dimensions often results in limited application of micro-milling. In the present study, electro discharge machining (EDM) is used for fabrication of micro-end mill tool. To ensure high dimensional accuracy of the tool, a parametric study is conducted by replicating the a tungsten carbide block to a tungsten carbide (WC) block. The relationships between the drilled cavities on the block and the features on the micro-tool are established. The influence of machining parameters (voltage, capacitance and spindle speed) on the response variables (entrance diameter, hole depth, material removal rate (MRR) and surface roughness) is reported. Capacitance is found more dominant as compared to other selected process parameters. Using optimized parameters from the parametric study, a WC micro-end mill tool of 100 µm diameter is fabricated. Channel of around 110 µm width, 40 µm depth and surface roughness of 70 nm is successfully fabricated on aluminum. The performance of the fabricated tool is compared with a commercial end mill tool by milling micro channels on stainless steel.

KEYWORDS

Micro-EDM; micro-milling; micro-end mill tool; MRR; surface roughness

Introduction

Micro-milling is a viable and economical choice for the fabrication of micro-channels (Koo et al., 2014), micro-fluidic devices (Guckenberger et al., 2015) and 3D micro-features. The size and accuracy of micro-features fabricated by micro-milling is significantly affected by micro-cutting tool. Fabrication of micro-cutting tool is difficult due to low strength. One of the most popular processes used for cutting tool fabrication is tool grinding. Grinding fails to make very small cutting tools because it exerts high force on the tool blank. It results in breakage of micro-tools due to less structural rigidity. However, ultrasonic vibration-assisted grinding proved its capability to reduce the tool diameter up to 20% of that of

CONTACT Ajay M. Sidpara ajaymsidpara@mech.iitkgp.ac.in Mechanical Engineering Department, Indian Institute of Technology Kharagpur, Kharagpur 721302, India.

normal process (Onikura et al., 2000). Electrolytic in process dressing has been used to make cylindrical tools with tip diameter of 1 μm (Ohmori et al., 2007). However, the dimensional accuracy and uniformity are affected by corner wear in the grinding wheel. Methods like laser beam machining or focused ion beam machining demand expensive machinery and sophisticated machining environments (clean room, vacuum chamber, etc.). Laser machining is employed to make cutting tools made of single crystalline diamond for machining of ceramic molds (Suzuki et al., 2013). Focused ion beam machining is known for making the smallest possible micro-cutting tools with complex geometries (Picard et al., 2003). However, during tool fabrication, more material is carved out from edge close to the ion source because of the nature of ion beam distribution. This results in rounded edges in tools fabricated by FIB. Moreover, material removal is very slow in FIB as it removes material atom by atom (Ding et al., 2008). Generally, all these processes demands sophisticated machinery with large investment in terms of machining environment and maintenance. This will add to the cost of cutting tool.

Electro discharge machining (EDM) can be a viable choice for processing micro-cutting tools as it is popular as a noncontact machining process. Melting and vaporization of the workpiece material are responsible for the material removal in EDM. The absence of contact between the tool and workpiece will reduce the chance of breakage during machining and the scrap rate falls down eventually. EDM has been used for fabricating micro-structures successfully by different researchers on various materials. Among the materials used for micro-cutting tools, tungsten carbide (WC) is comparatively cheaper and exhibits good machining performance (Adams et al., 2001). Yan et al. (1999) drilled micro-holes in tungsten carbide workpiece using copper tool electrodes to investigate the effects of electrode polarity, tool rotational speed and tool electrode geometry. It is observed that the increase in tool rotation speed helps to reduce the expansion of hole diameter if a notch is provided for the cylindrical tool for enhanced dielectric flushing. The effect of electrode polarity differs in different combinations of tool and workpiece material. While machining WC with copper electrode, positive polarity to the tool electrode has produced better surface characteristics. A micro-slit die with 15 micro fins for fabricating micro-heat sink is machined using EDM on WC blank (Wang et al., 2005). The change in average slit width (ASW) and average slit depth (ASD) for different combinations of voltage, pulse duration and dielectric flushing pressure are measured. ASD and ASW are increased with pulse duration within a range because of increase in discharge energy but decreased beyond that range due to inadequate debris removal and unstable discharges. Setting the open voltage to the highest values resulted in more debris formation and high side sparking which led to large amount of wear in the copper foils. Han et al. (2006) investigated the feasibility of fabricating sub micro-meter structures. It is observed that the accuracy of positioning, geometrical errors and minimum possible discharge energy are the limiting factors for employing EDM for sub micro-machining. In this study, WC is suggested as a better workpiece material than tungsten because of better material structure.

Over the years, performance analysis of micro-EDM variants on a large variety of materials is done by various research groups (Jabbaripour et al., 2012; Karthikeyan et al., 2014; Habib and Okada, 2016). A comparative study is conducted to analyze the effect of RC type and transistor type pulse generator on the quality of machined structures in WC (Jahan et al., 2009). It is observed that RC pulse generators outperform transistor type while drilling micro-holes in WC. Resolution of micro-EDM can be improved with using RC type pulse generators as the discharge energy can be controlled more easily in the lower range. Discharge conditions in micro-EDM drilling of WC is studied by various researchers (Tak et al., 2009; Jahan et al., 2012). The machining experiments are designed for various capacitance and resistance values. From the analysis of Tak et al. 2009, it is found that the combination of capacitance 50 pF and resistance 3.3 kΩ is the optimum discharge condition as the increase in resistance reduces effective machining voltage between workpiece and tool. The effect of tool rotational speed, polarity of electrode along with the gap control parameters on material removal rate (MRR) and tool wear rate (TWR) during micro-EDM of WC are investigated (Jahan et al., 2012; Jafferson et al., 2016). Tool rotation speed influences the MRR and tool wear in a proportional manner as the debris removal becomes more efficient with increase in tool rotational speed. It is revealed that apart from discharge energy, the melting point and electrical and thermal conductivity of the tool electrode material also influence the quality of surfaces produced with EDM. Performance analysis of powder mixed EDM on WC alloy has been conducted (Sharma and Singh, 2016). It has been concluded that pulse on time, powder composition and discharge current can be considered as the most influential parameters in machining of WC.

Figure 1 shows the shapes of micro-end mill cutters fabricated by different strategies. From this, it is clear that instead of miniaturizing the conventional tool geometries, most of the researchers focused in fabrication of micro-cutting tools with simple geometry (D-shaped tool, triangle shaped tool, semi sphere shaped tool, cone shaped tool, hexagonal tools, rectangular tools, etc.). Among these tool geometries, the tools with a straight edge will have high positive rake angle which adversely affect the cutting performance. D-shaped or semi sphere shaped tools will exert a large rubbing force on the micro-channel walls whereas the conical tools fail to achieve the shape accuracy.

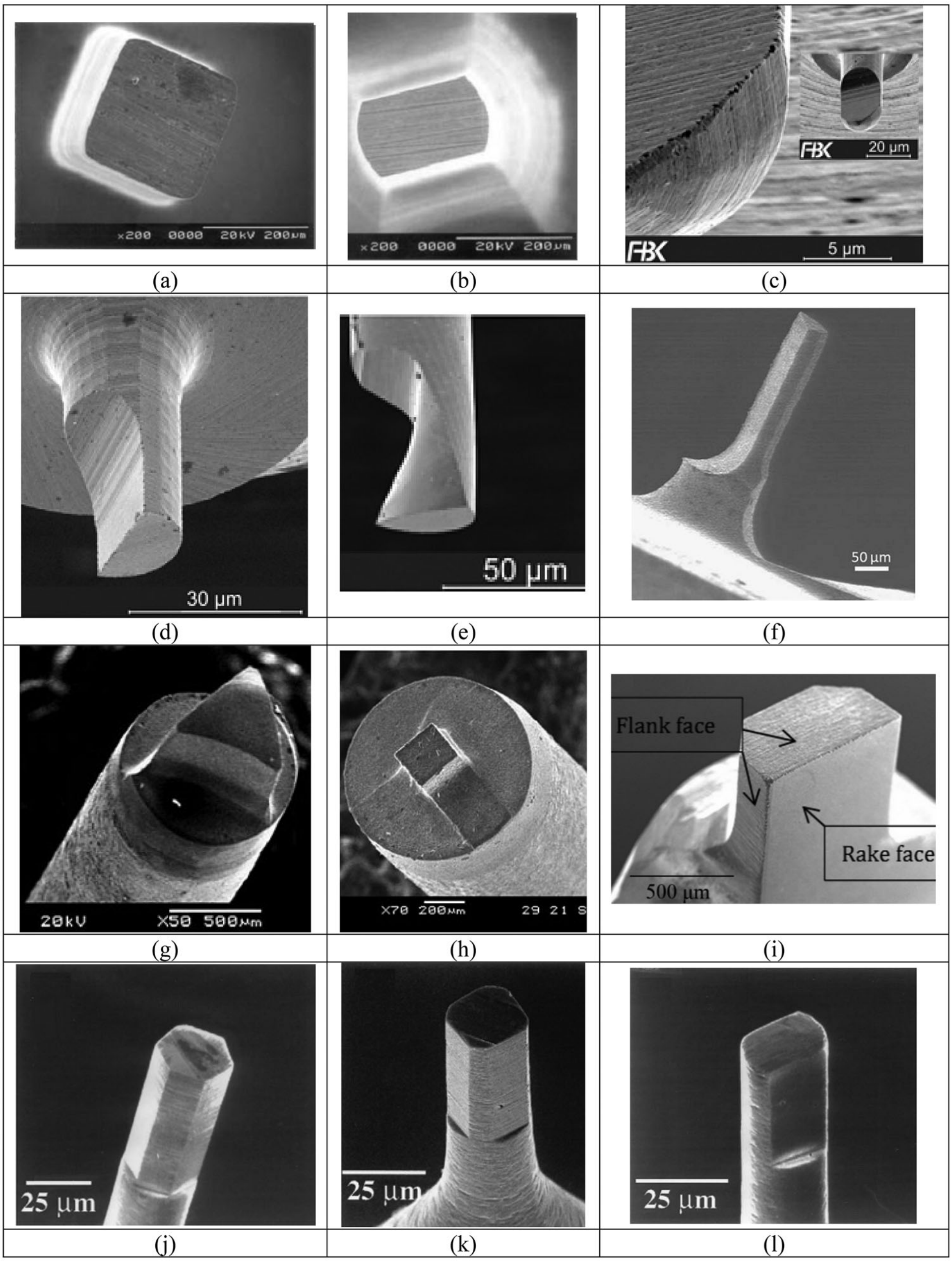

Figure 1. Micro-end mill tools fabricated by different micro-fabrication methods. **(a, b)** electrolytic in-process dressing (Lee et al., 2002) **(c, d, e)** tool grinding (Aurich et al., 2012), **(f)** wire EDG (Fleischer et al., 2008), **(g, h)** block EDG, **(i)** wire EDM and grinding (Zhan et al., 2015), **(j, k, l)** focused ion beam machining (Adams et al., 2001).

EDM has been used for fabricating micro-cutting tools with different strategies. Most of them relied upon wire EDM to shape the workpiece to the intended geometry. Perveen et al. (2012) utilized block electro discharge grinding (EDG) to make micro-tools with different shapes (D-type, triangular type and square type) and compared the tool geometries by conducting machining experiments. Wire electro discharge grinding is used to fabricate gun barrel type cemented WC drilling tools (Egashira et al., 2011). WC micro-tools are fabricated with wire EDM by Chern et al (2007). Polycrystalline diamond micro-tools are successfully fabricated with high accuracy by wire EDG utilizing the principle of graphitization of diamond grains at low discharge energy conditions (Fonda et al., 2012). Compared to the above mentioned strategies, micro-EDM milling and drilling have the advantages of better MRR, flexibility and capable of machining complex 3D structures (Morgan et al., 2004). When the cutting tool size reduces to 100 μm or less, tool rigidity reduces significantly. Hence, a simple tool geometry without flutes can perform the cutting action and retain the sharpness of the cutting edge for a longer time. The tools fabricated by Perveen et al. (2012) exhibit high cutting force during machining due to large negative rake angle and constant rubbing of some parts of the tool during machining. This will eventually result in early tool breakage. Kawasaki et al. (2013) examined the possibility of using square end mill in cutting of molding die by providing inclination to the tool axis. Preliminary experiments are performed to fabricate four edged WC end mill tool by micro-EDM along with EDG and it is used for machining of micro-channel on PMMA (Ganesh et al., 2017).

Table 1 summarizes the literature on micro-tool fabrication methods. It is observed from the literature that use of micro-EDM drilling is not much explored for fabrication of micro-end mill tools. Hence, in the present study, a parametric analysis is performed to get better dimensional control of end mill tool. A four edged WC end mill tool is fabricated and evaluated its performance by machining of micro-channel on aluminum and SS 304L.

Experiment details

A 3 axis micro-EDM machine tool (Mikrotools, Singapore) with RC type pulse generator is used for performing the machining experiments. Details of the experiment are given in Table 2. Being the most popular cutting tool material for end mill tools, WC is selected as the workpiece material. To reduce the machining errors due to tool wear during EDM, the tool material is also chosen as WC rods. The experiments are designed with a 300 μm diameter tool electrode and 50 mm × 12 mm × 12 mm WC block. The curvature of the EDM tool electrode can be replicated as the cutting edges of the end mill tool. This curvature will help to keep the effective rake angle positive. Moreover, compared to two flute end mills, this tool will have greater rigidity as more material is available. However, high

Table 1. Micro-cutting tool fabrication methods and details.

Author	Tool fabrication method	Tool material	Tool shape/ Tool diameter	Remarks
Ding et al. (2008)	FIB	Single crystal diamond	25 µm (cutting edge length)	Micro-milling experiments on Al 6061
Wang et al. (2016)	Electroplating	CBN coated tungsten carbide	300 µm	Simultaneous Milling and grinding tool
Fleischer et al. (2008)	Wire EDG	–	Single edge/100 µm Helical/ 50 µm	Stability simulations by FEM analysis
Perveen et al. (2012)	Block EDG	Poly crystalline diamond (PCD)	D/ triangle /square shaped ∼200 µm	D shaped tool is shown better performance
Onikura et al. (2000)	Ultrasonic grinding	Cemented carbide	Flat drills/ 17 µm	For tensile grinding force, tool is broken easily
Nakamoto et al. (2012)	Wire EDM	PCD	Special shape/ 100 µm	Machining experiments on tungsten carbide
Morgan et al. (2004)	Wire EDG and block EDG	PCD	Cylindrical/ 50 µm	Micro-milling experiments on soda lime glass
Adams et al. (2001)	FIB	PCD	Special shape with ∼25 µm wide features	Machining experiments on PMMA, Al6061, steel 4340 and brass
Cheng et al. (2010)	Wire EDM	PCD	Straight edge end mill	Straight edge end mill tools with small rake angles have greater stiffness and lower tool wear
Picard et al. (2003)	FIB	Tungsten carbide/ HSS/ diamond	Different shapes 15-100 µm	Micro-grooves of 40-0150 µm pitch machined on a 3 mm polymer rod
Zhang et al. (2013)	Wire EDG	PCD	∼400 µm	Semi-spherical tools for making high precision dimples tungsten carbide
Chern et al. (2007)	Wire EDG	Tungsten carbide	100 µm	Micro-slot and thin-walled micro-structure fabricated on Al 6061-T6
Fonda et al. (2012)	Wire EDG	PCD	Hexagonal shape tool ∼500 µm	Optimization of PCD micro-cutting tool fabrication using wire EDM

Table 2. Experiment details.

Tool electrode (−ve)	WC (50 mm × 12 mm× 12 mm)
Workpiece material (+ve)	WC (300 µm dia.)
Dielectric fluid	EDM-3 oil
Feed rate	0.2 mm/min

dimensional accuracy and shape accuracy will be a challenge while fabricating cutting tools with micro-EDM. Considering the difficulty of imaging and measurements, the process is replicated on a block for simplicity as shown in Figure 2. While fabricating the tool, the dimensions of the cavities control the dimensions of the cutting tool. The depth of the cavity will be replicated as length of cutting tool. The final cutting tool diameter will be affected by the increase in diameter of the cavity due to side sparking. Examining the geometry of the machined cavity will help to understand the geometrical errors in the cutting tool and select the appropriate level of EDM parameters.

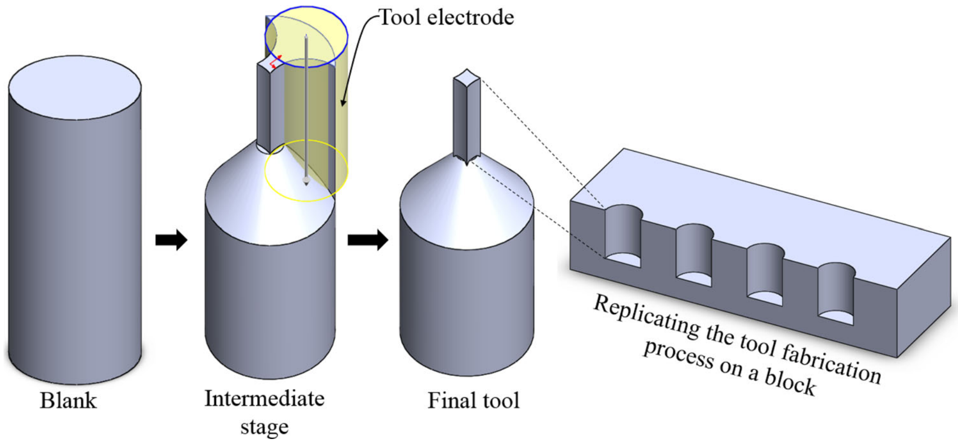

Figure 2. Replicating the tool fabrication process on a block.

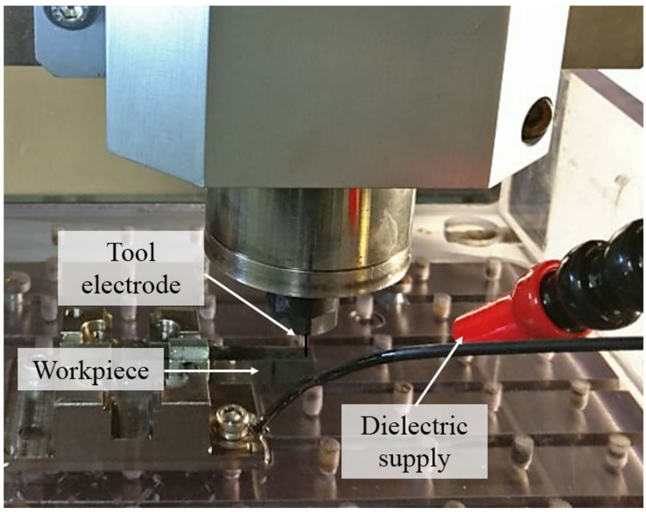

Figure 3. Experimental set up on EDM machine.

The experimental set up is shown in Figure 3. To have a cutting tool of uniform height and high dimensional accuracy, the difference between the designed values of depth and diameter of the cavity with the actual values should be minimum. To determine the effect of machining parameters on entrance diameter, hole depth, MRR and surface roughness, an experimental plan is prepared using Box–Behnken design (Ferreira et al., 2007). Voltage, capacitance and tool rotation speed are selected as independent parameters and their levels are given in Table 3. Total 17 experiments are planned as per the design with different combinations of the independent process parameters as given in Table 4. Capacitance values cannot be changed uniformly so that discrete coded values as given in the machine are used in the experimental design. Response parameters entrance

Table 3. Machining paraeters and levels.

Parameter	Level Low	Middle	High
Voltage (V)	80	100	120
Capacitance (machine setting/actual (nF))	2/0.1	4/10	6/400
Spindle speed (RPM)	200	1500	2800

Table 4. Experimental design for parametric analysis.

Expt. No	Voltage V	Capacitance Machine setting/ (actual, nF)	Speed RPM	Entrance dia. µm	Hole depth µm	MRR mm^3/ min ($\times 10^{-3}$)	Surface roughness (R_a) µm
1	80	2 (0.1)	1500	325	980	0.313	0.139
2	120	2 (0.1)	1500	335	969	0.6	0.183
3	80	6 (400)	1500	354	773	2.3	0.902
4	120	6 (400)	1500	370	742	3.2	0.943
5	80	4 (10)	200	345	916	1.1	0.437
6	120	4 (10)	200	349	904	2.2	0.691
7	80	4 (10)	2800	333	902	1.7	0.422
8	120	4 (10)	2800	343	854	2.8	0.6
9	100	2 (0.1)	200	338	954	0.4	0.215
10	100	6 (400)	200	374	750	3.2	0.921
11	100	2 (0.1)	2800	317	985	0.6	0.151
12	100	6 (400)	2800	384	749	3	0.915
13	100	4 (10)	1500	342	916	2	0.302
14	100	4 (10)	1500	338	908	2.3	0.321
15	100	4 (10)	1500	332	911	2.4	0.356
16	100	4 (10)	1500	335	904	2.2	0.406
17	100	74 (10)	1500	338	927	2.1	0.378

diameter, hole depth, MRR and surface roughness (Ra) are also reported in Table 3 which are used for getting Equations (1)–(4).

After drilling each cavity, the bottom surface of the tool electrode is flattened by EDG process to reduce the effect of tool wear on the subsequent drilling process. Machining time for drilling each cavity is recorded. After the machining experiments, the depth and width of the cavities are measured using SEM. To measure the volume of material removal, SEM images of the cavities are exported to SolidWorks® software and the volume data of the cavities are generated as shown in Figure 4. This volume is divided by the machining time for each experiment to get the MRR in mm^3/min for each cavity. Figure 5 shows the method of measuring average surface roughness (R_a) of the wall of the cavity. The R_a values are taken at the center of the channel for a length up to 300 µm from the top of the channel to ensure consistency in measurement length as the cavity depth varies noticeably in different experiments.

Tables 5 and 6 show analysis of variance (ANOVA) all 4 response parameters. Factors with the p value less than 0.05 are considered as significant at 95% confidence level. Applicability of the model for predicting the response characteristics is evaluated using Lack of fit, adjusted R^2 value and predicted R^2 value. As the lack of fit is not significant ($p\ value > 0.05$),

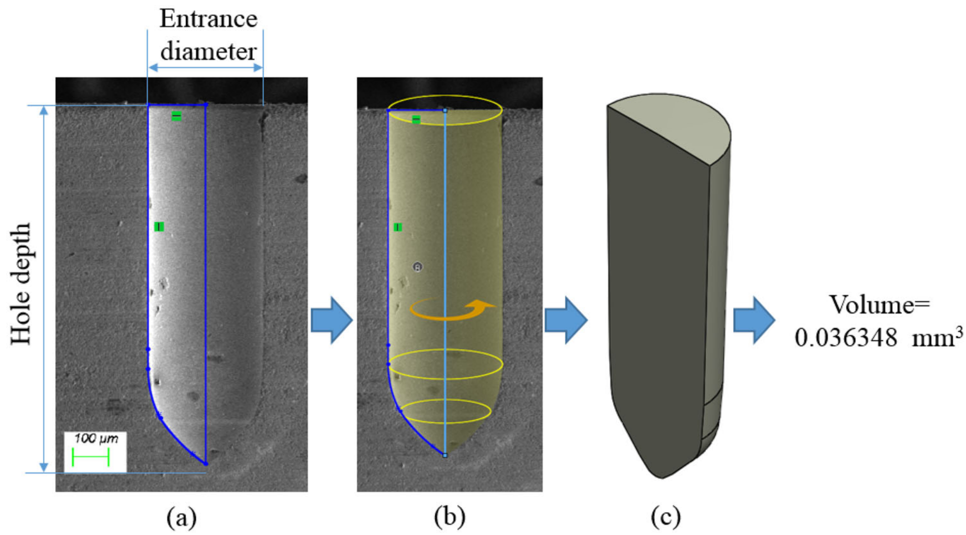

Figure 4. Method of generating volume data for MRR calculation (V = 100, C = 0.1 nF and S = 2800 RPM).

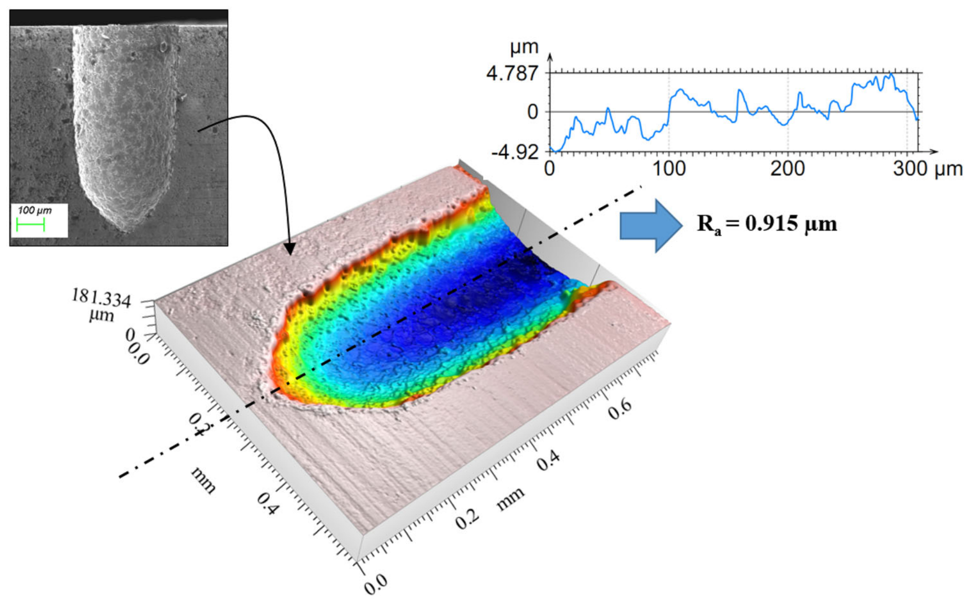

Figure 5. Sample measurement of surface roughness on the inner walls of the cavity (V = 100, C = 400nF and S = 2800 rpm).

adjusted R^2 and predicted R^2 values are close to each other for all the responses, it is clear that the model is suitable for analyzing the process parameters. Table 7 shows the percentage contribution of each independent parameter on the response variable calculated using the ANOVA tables (Tables 5 and 6) which concludes that capacitance is the most significant factor which affects the quality of the tool followed by voltage and speed.

Table 5. ANOVA of entrance diameter and hole depth.

Entrance diameter			Hole depth		
Source	*F* value	*p* value Prob > *F*	Source	*F* value	*p* value Prob > *F*
Model	13.99	0.0011	Model	56.06	<0.0001
A-Voltage	5.21	0.0463*	A-Voltage	6.07	0.0432*
B-Capacitance	94.17	<0.0001*	B-Capacitance	454.54	<0.0001*
C-Speed	2.91	0.1318	C-Speed	0.7382	0.4187
AB	0.2699	0.6194	AB	0.4483	0.5246
AC	0.2503	0.6322	AC	1.61	0.2450
BC	6.47	0.0384*	BC	1.29	0.2938
A^2	0.1625	0.6989	A^2	0.7920	0.4030
B^2	11.21	0.0123*	B^2	33.63	0.0007*
C^2	4.60	0.0693	C^2	3.29	0.1125
Lack of fit	13.99	0.0794	Lack of fit	4.83	0.0811
R^2	0.9783		R^2	0.9746	
Adjusted R^2	0.9614		Adjusted R^2	0.9630	
Predicted R^2	0.9147		Predicted R^2	0.9045	

*Significant terms.

Table 6. ANOVA of MRR and surface roughness.

MRR			Surface roughness		
Source	*F* value	*p* value Prob > *F*	Source	*F* value	*p* value Prob > *F*
Model	33.85	<0.0001	Model	44.26	<0.0001
A-Voltage	29.31	0.0010*	A-Voltage	10.33	0.0148*
B-Capacitance	248.99	<0.0001*	B-Capacitance	346.35	<0.0001*
C-Speed	3.30	0.1122	C-Speed	1.20	0.3100*
AB	2.20	0.1816	AB	0.0007	0.9797
AC	0.0090	0.9271	AC	0.4466	0.5254
BC	1.06	0.3371	BC	0.2601	0.6257
A^2	6.16	0.0421*	A^2	10.10	0.0155*
B^2	12.28	0.0099*	B^2	13.30	0.0082*
C^2	0.0680	0.8018	C^2	12.21	0.0101*
Lack of fit	6.13	0.0562	Lack of fit	2.94	0.1625
R^2	0.9668		R^2	0.9810	
Adjusted R^2	0.9517		Adjusted R^2	0.9696	
Predicted R^2	0.9033		Predicted R^2	0.9371	

*Significant terms.

Results and discussion

Total 17 cavities are machined according to the experimental plan with different machining parameters. Figure 6 shows scanning electron microscopy (SEM) images of the front face of the machined cavities. It is observed that the surface quality, cavity profile and dimensions of cavities have noticeable difference. As the capacitance and voltage values moves to the extreme settings, the hole broadens, depth decreases and quality of surface diminishes. This trend is systematically analyzed by studying the effect of each process parameter on the response variable with the help of ANOVA study (Montgomery, 2008). Regression equations (Equations (1)–(4)) are obtained after dropping insignificant terms for each response parameter and used for plotting the surface graphs.

Table 7. Contribution of the selected parameters.

	% Contribution			
Parameters	Entrance dia.	Hole depth	MRR	R_a
Capacitance (B)	92.06	98.52	88.42	96.78
Voltage (A)	5.09	1.31	10.41	2.89
Speed (C)	2.84	0.16	1.172	0.34

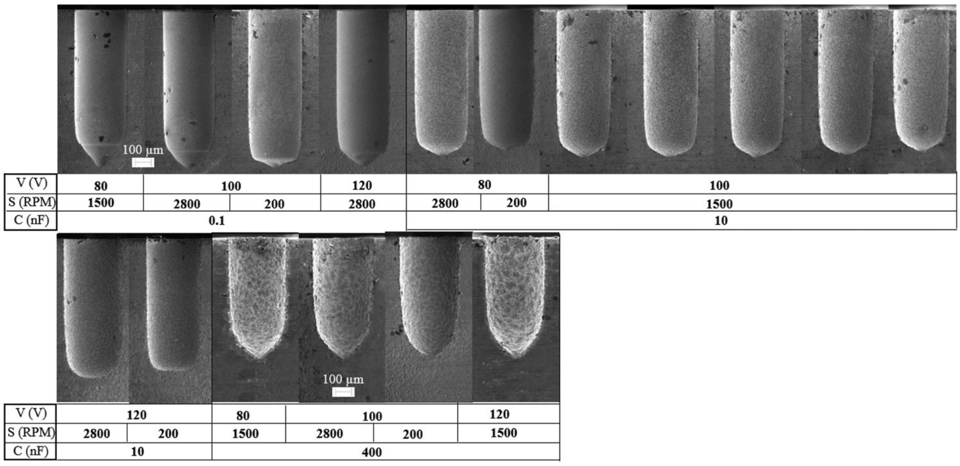

Figure 6. SEM images of the cavities drilled with different levels of machining parameters.

Entrance diameter

Diameter of the entrance section has very much importance in deciding the geometry and dimensions of the final cutting tool. Entrance diameter is taken as an indirect measure of the overcut distance in micro-EDM drilling. As the overcut increases, the diameter of the hole increases and more material will be taken out from the cutting tool surface during tool fabrication. This will result in a smaller cutting tool as shown in Figure 7(a). Entrance diameter 1 is the same as the diameter or the tool electrode and Entrance diameter 2 includes overcut. The relationship between the machining parameters and the entrance diameter is given by Equation (1).

$$\begin{aligned} \mathit{Entrance\ diameter} = {} & 0.34 + 0.00024 \times V + 0.013 \times C - 0.000026 \\ & \times S + 2.99E - 06 \times C \times S + 0.0024 \\ & \times C^2 + 3.74E - 09 \times S^2 \end{aligned} \tag{1}$$

Value of coefficient of determination (R^2) close to 1 implies good agreement of experimental data and equation. Equation (1) has R^2 value 0.9783 which can be used as an empirical relation to calculate entrance diameter of cavity or final cutting tool diameter.

To analyze the effect of each machining parameter on entrance diameter, a response surface curve is plotted as given in Figure 8. It is evident from

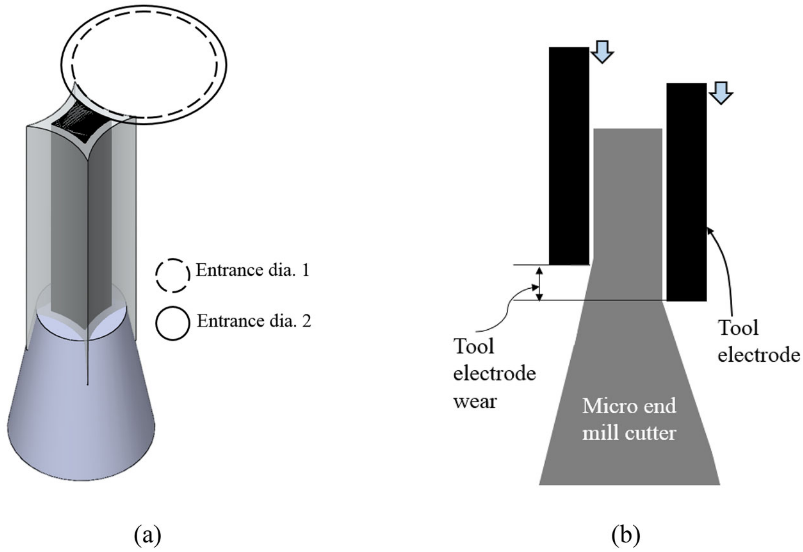

Figure 7. Effect of (a) entrance diameter and (b) hole depth on final end mill tool dimensions.

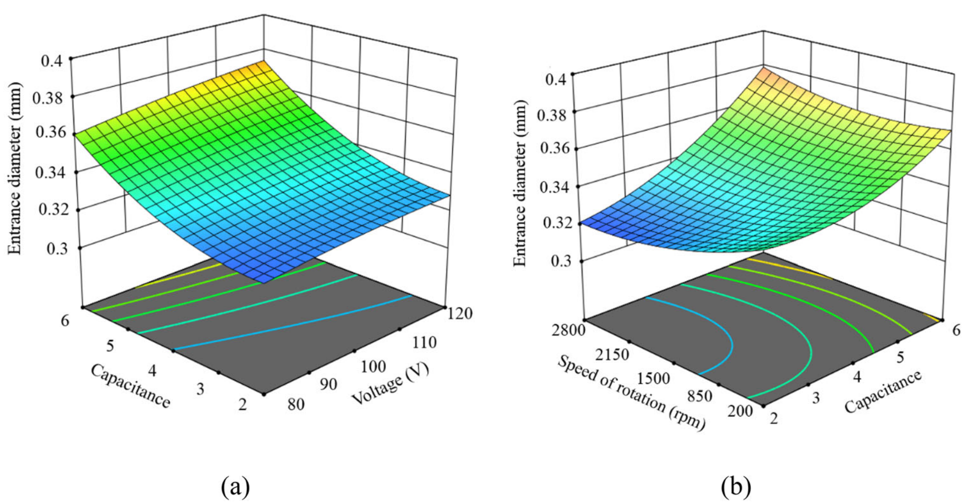

Figure 8. Effect of (a) capacitance and voltage (b) speed and capacitance on the Entrance diameter.

Figure 8a and b that capacitance is the most important factor affecting the entrance diameter. As capacitance increases, discharge energy increases and more material is carved out from the side walls due to side sparks. This will increase the debris concentration in the area between the tool and side wall of the hole. These debris particles will eventually reduce the effective resistance of the dielectric and produces secondary sparks. Arcing and shorting will increase and the process becomes more unstable. All these events will lead to broadening of the hole diameter. Voltage is the second

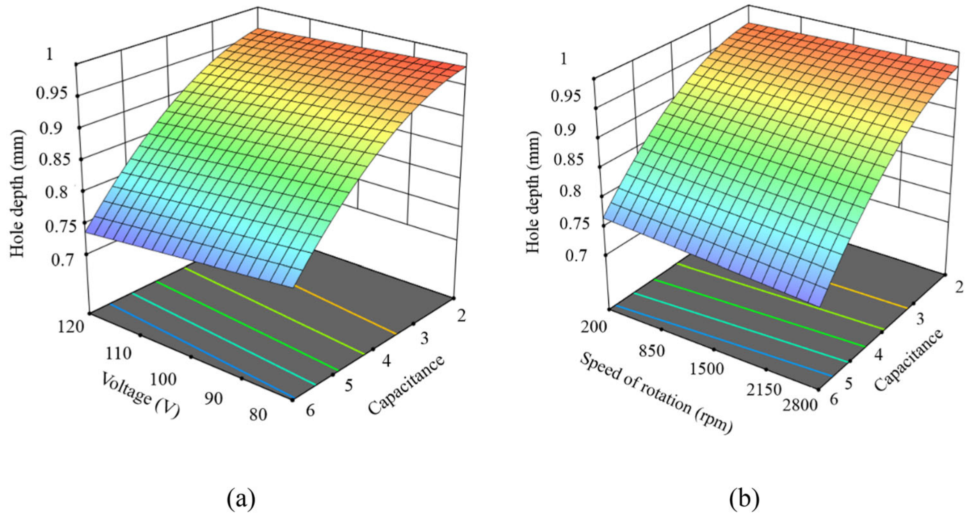

Figure 9. Effect of (a) capacitance and voltage (b) speed and capacitance on the hole depth.

significant factor which controls the overcut. It has less effect on the low capacitance side but as it moves to the extreme capacitance values, it contributes to the increase in diameter of the cavity. Figure 8b shows the effect of spindle speed along with capacitance. As the spindle speed increases, debris particle will be thrown out of the machining zone easily and the side walls will be always exposed to continuous discharges, which may increase the overcut time to time. However, this factor does not have much influence on the diameter of the cavity as compared to capacitance and voltage.

Hole depth

This is an important parameter in the tool fabrication process which determines the effective cutting length of the end mill tool. Inability to plunge the tool electrode to a constant depth will result in unsymmetrical tool shape as shown in Figure 7b. This will reduce available cutting length. Equation (2) shows the empirical relation between the machining parameters and hole depth having $R^2 = 0.9746$. It is observed from Figure 9a and b that capacitance has significant effect on the hole depth. Discharge energy increases with increase in capacitance and it results in more MRR from the workpiece as well as tool. High wear of the tool electrode results in lengthwise erosion of the tool. When tool reaches to 1 mm intended (programmed) depth, tool length is reduced due to lengthwise wear and it increases the difference between the intended depth and actual machined depth of the hole. Voltage and tool rotational speed do not have prominent effect. However, selecting lower value of voltage along with low capacitance and high tool rotational speed will result in depth of hole

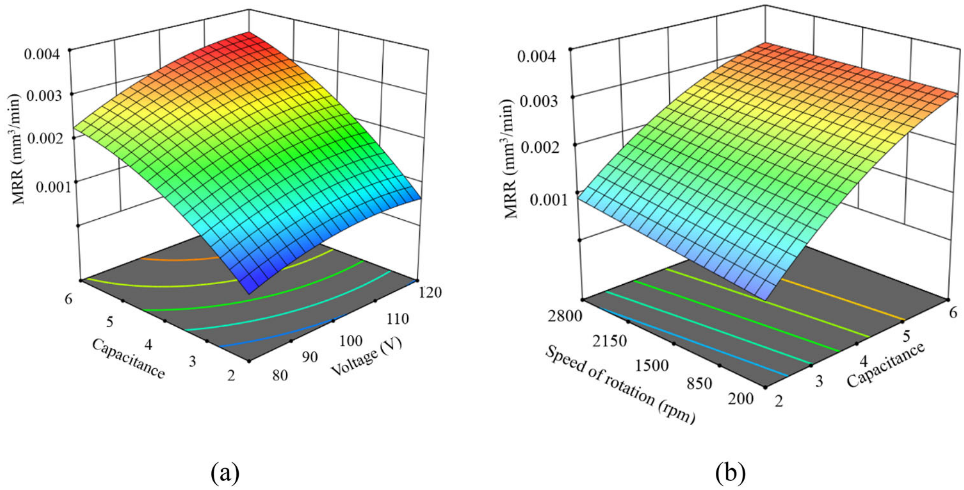

Figure 10. Effect of (a) capacitance and voltage (b) speed and capacitance on MRR.

very close to the intended depth. This equation can be used to predict the tool wear for a particular parameter setting during micro-tool fabrication. Furthermore, these values can serve as an input to the tool compensation algorithm to predict the actual tool travel distance for drilling intended hole depth. Thus, a micro-tool with intended length of cut can be fabricated.

$$\textbf{Hole depth} = 0.97 - 0.0001 \times \mathrm{V} + 0.029 \times \mathrm{C} + 0.000032 \times \mathrm{S} - 3.53\mathrm{E}-07 \times \mathrm{V} \times \mathrm{S} - 0.010 \times \mathrm{C}^2 \tag{2}$$

Material removal rate

MRR is calculated by dividing the volume of the cavity with the machining time as explained earlier. MRR depends on hole depth and diameter of the cavity. The effect of machining parameters on MRR is expressed as an empirical relation as shown in Equation (3) having $R^2 = 0.9668$.

$$MRR = -0.0091 + 0.00014 \times V + 0.00097 \times C + 1.09E - 07 \times S + 4.12E - 06 \times V \times C - 6.75E - 07 \times V^2 - 0.000095 \times C^2 \tag{3}$$

Figure 10 shows the effect of the selected process parameters on MRR. It is observed that capacitance has the highest effect on MRR as compared to voltage and tool rotational speed. This can be explained by the smaller machining time, and increased diameter of the cavity because of high energy discharges. However, as the capacitance level tends to reach the highest level, MRR reduces. This can be due to several factors. One of them is the presence of abundant debris particles because of the increase in material removal results in large amount of shorting during machining.

This will eventually decreases the MRR. Other possible reason is the reduced volume of the cavity due to tool electrode wear. Tool electrode is getting worn significantly lengthwise which results in shallow cavity. As explained before, MRR is a function of diameter and depth of the hole. For high capacitance values, even though the diameter of the hole increases, reduction in depth becomes prominent and the volume of the cavity reduces. At the extreme capacitance points, this will cause a reduction in the rate of material removal. Predicting MRR for drilling a single cavity using Equation (3) will help to calculate the approximate tool fabrication time for micro-end mill tools with different diameter and length of cut.

Surface roughness

Surface roughness is an important parameter of the cutting tool. Low surface roughness reduces friction during flow of chip over the rake surface and prolongs the tool life. It is evident from Figure 6 that the machining parameters severely affect the quality of the machined surface. The surface quality is quantified in terms of surface roughness parameter R_a. The relationship between the roughness value and machining parameters is obtained by Equation (4) ($R^2 = 0.9809$) as given below,

$$\begin{aligned} \textit{Surface roughness}, R_a = 2.04 - 0.040 \times V - 0.015 \times C - 0.00018 \\ \times S + 0.00022 \times V^2 + 0.025 \times C^2 + 5.72E - 08 \times S^2 \end{aligned} \tag{4}$$

Figure 11a and b shows that surface roughness increases significantly with increasing capacitance. High capacitance increases discharge energy and it results in bigger size crater. Surface roughness is affected by the peaks and valleys of the surface. Due to bigger craters, peaks and valleys increase and results in high surface roughness. Increase in voltage also results in increase in surface roughness but the amount of change is very less. Tool rotational speed helps to remove debris from the working zone and allow a fresh surface to participate during subsequent sparking. It also distributes the sparks evenly on the surface during tool rotation. Hence, chances of formation of recast layer reduces. However, tool rotational speed does not have significant effect on surface roughness independently.

Based on the parametric study, optimum combination of the selected parameters is found out by the method reported by Derringer and Suich (1980) which is used for simultaneous optimization of several response variables. The optimization is performed in terms of desirability function (di). The desirability function involves transformation of each estimated response variable (entrance diameter, hole depth, MRR and surface roughness) to a desirability value di, where $0 \leq \text{di} \leq 1$. The value of di increases

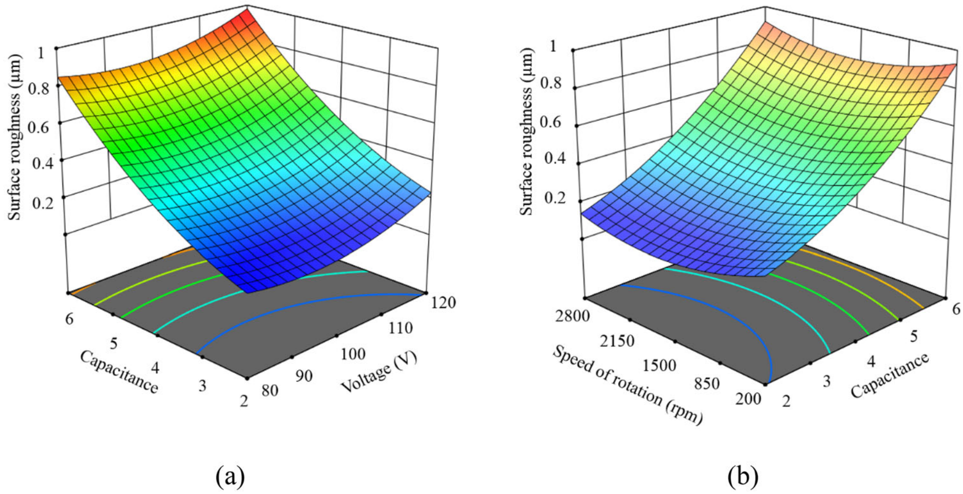

Figure 11. Effect of (a) capacitance and voltage (b) speed and capacitance on the surface roughness.

as the "desirability" of the corresponding response increases. The all desirability values are then combined using the geometric mean as given by Equation (5). This single value of D gives the overall assessment of the desirability of the combined response levels. Levels of the factors which exhibit maximum desirability values (close to 1) are chosen as the final combination of machining parameters.

$$D = (d_1 x\ d_2 x\ \ldots\ldots x\ d_k)^{1/k} \tag{5}$$

where k is number of response variables.

The objective function is bounded by the constraints of maximizing the hole depth, maximizing MRR, minimizing the entrance diameter and minimizing the surface roughness. However, the factors that directly affect the geometry and quality of the final tool (hole depth, entrance dia. and surface roughness) has given more weightage compared to the MRR. From this method, voltage = 99 V, capacitance = 3 (1 nF) and spindle speed = 2573 rpm produce a cavity of entrance dia. = 0.3225 mm, hole depth = 0.9567 mm, MRR = 0.0014 mm^3/min and surface roughness, R_a = 0.165 μm with a desirability value of 0.919.

Fabrication of micro-end mill tool

Based on the optimum level of the process parameters found in the previous section, a micro-end mill tool with four cutting edges is fabricated. The micro-tool is modeled in Solidworks® for a diameter of 80 μm and the EDM tool path for tool plunging is written accordingly. A 300 μm WC rod is used as the EDM tool electrode and a commercially available 500 μm

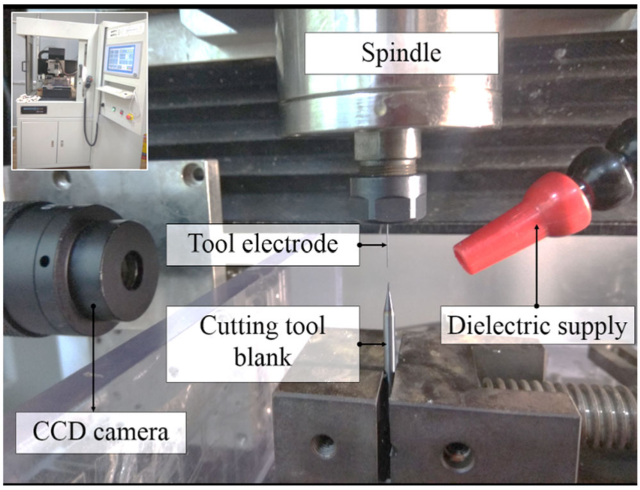

Figure 12. EDM set up for micro-end mill tool fabrication.

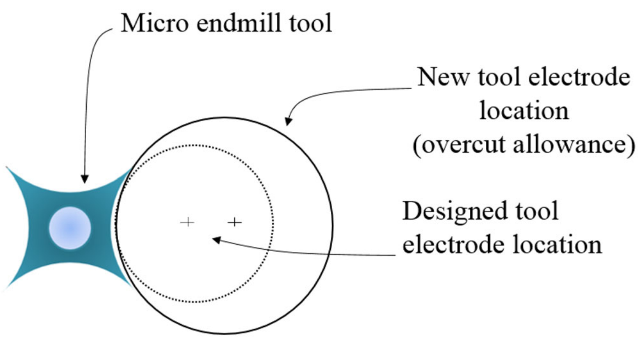

Figure 13. Re-designing the tool path for EDM tool using predicted overcut.

end mill tool as cutting tool blank. The top surface of the blank is flattened to remove the existing cutting edges and the designed profile is cut on tool blank using the proposed method. Experimental set up for micro-end mill fabrication is given in Figure 12. The prediction for entrance diameter (0.3225 mm) corresponding to optimum machining conditions is used during the tool fabrication to offset the plunging location of the tool to provide the overcut allowance as shown in Figure 13. This will help to reduce the effect of errors in tool dimensions due to overcut during EDM.

Figure 14 shows the SEM images of the fabricated tool having included angle is near to 79°. The available cutting length of the tool is 955.41 µm which is very close to the predicted hole depth (956.7 µm) by optimization method. Effectiveness of overcut allowance is visible as it could achieve the tool diameter of 80 µm. This shows that the optimum parameters are capable of fabricating a tool with intended geometry. Edge radius of the tool is around 1.113 µm which is in the range of edge radius of commercially available tools (Uhlmann et al., 2016). However, long tools with very small

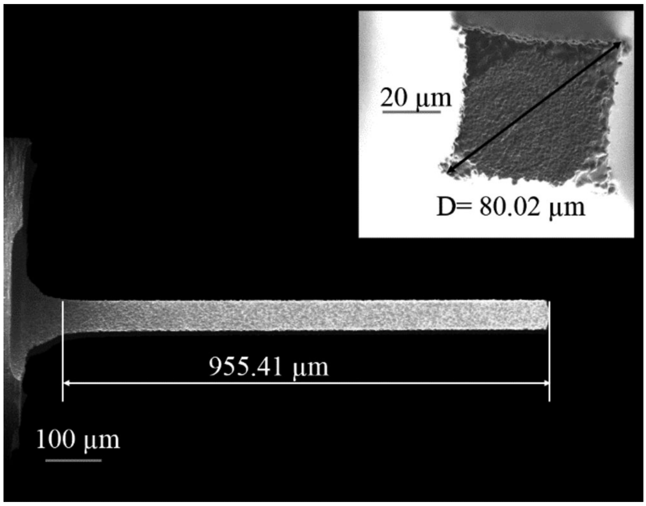

Figure 14. Micro-end mill tool fabricated using the optimum process parameters (inset figure shows top view of the tool).

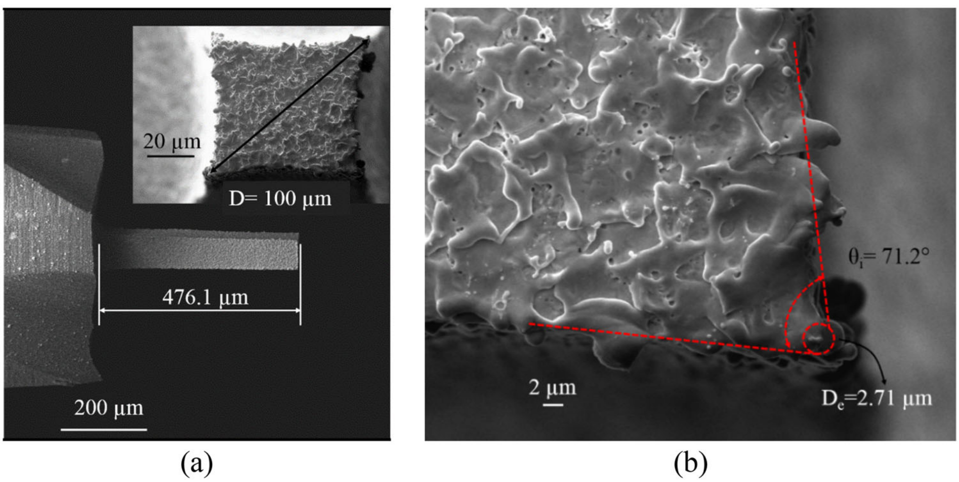

Figure 15. (a) Micro-end mill tool fabricated for milling experiment and (b) cutting edge geometry of micro-tool

dimensions are prone to easy breakage during machining. To conduct some machining experiments, a shorter tool of 100 µm diameter and around 476 µm length is fabricated using the same method. As shown in Figure 15, this tool also exhibits high dimension accuracy and straightness along length of cut.

A 3 axes micro-milling machine (KERN Evo, Germany) is used to evaluate the performance of the fabricated tool as shown in Figure 16. Micro-channel of 18 mm length is fabricated on aluminum 6061. Machining parameters are fixed as given in Table 8. A piezoelectric dynamometer (KISTLER, 9119AA2) is used to monitor the cutting forces and breakage of

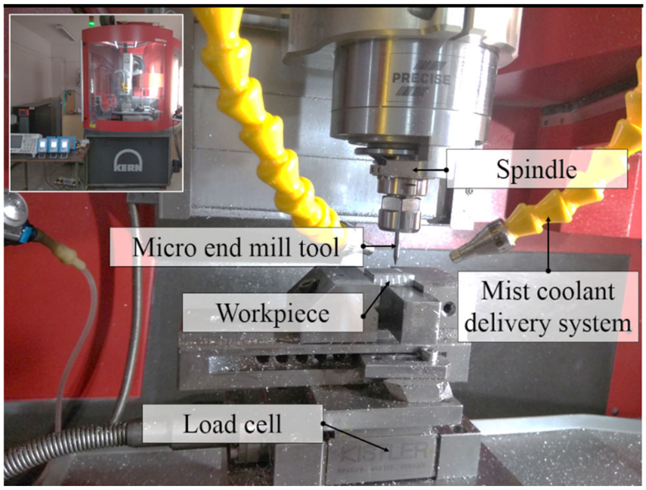

Figure 16. Milling set up for performance evaluation of fabricated micro-end mill tool.

Table 8. Machining parameters cutting micro-channels using fabricated micro-end mill tool.

Workpiece	Aluminum 6061
Tool	Tungsten carbide (100 μm)
Spindle speed	15,000 rpm
Feed rate	2 mm/min
Coolant	Mist coolant

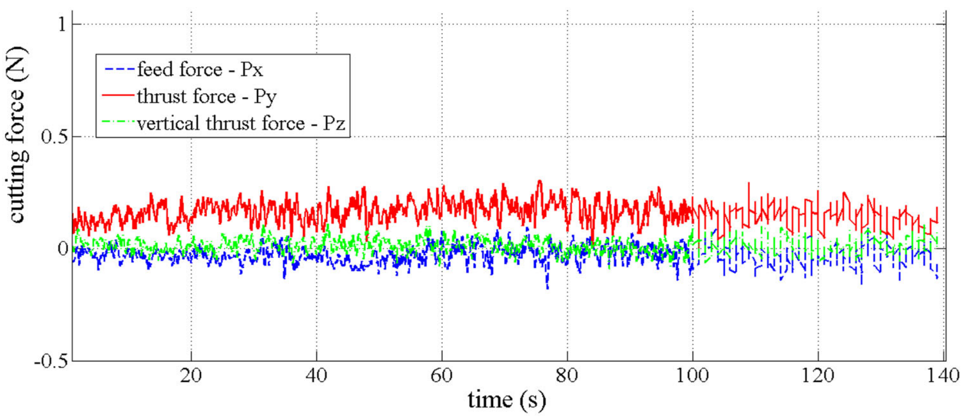

Figure 17. Cutting force measurement data during milling with the fabricated tool.

the cutting tool. Figure 17 shows force signal during machining. Root mean square values of the feed force (P_x), thrust force (P_y) and vertical thrust force (P_z) are 0.0507 N, 0.1659 and 0.0348 N, respectively. It is also observed from the force signal that all the forces are stable with in a range. Hence it is confirmed that the cutting tool is stable during machining.

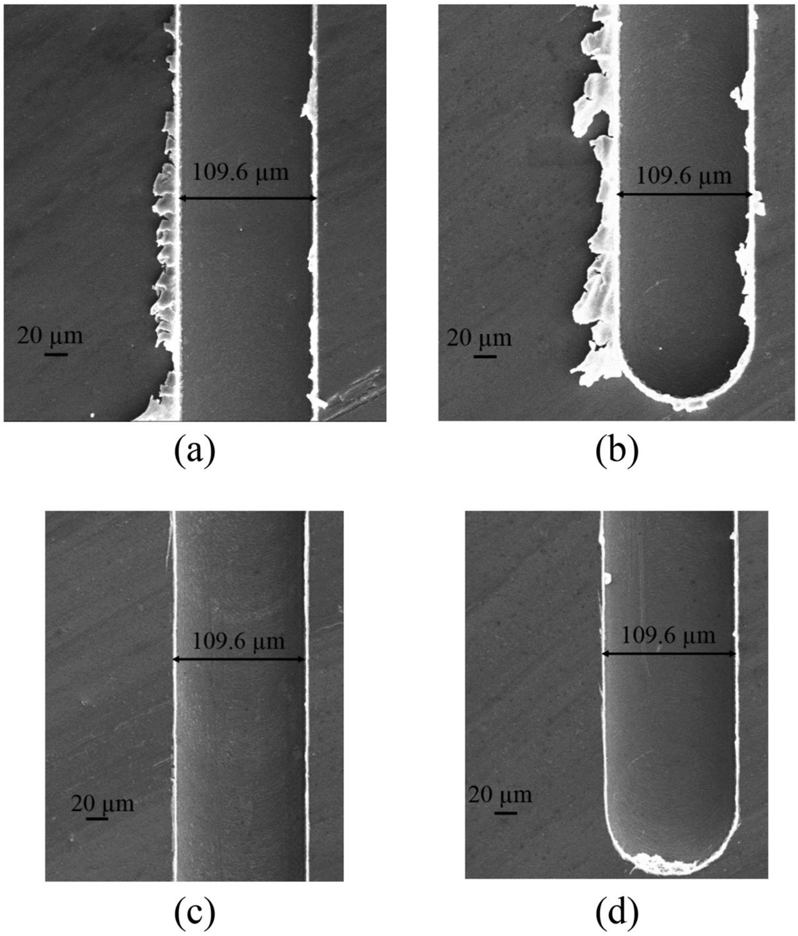

Figure 18. SEM images of (a) entrance section and (b) exit section of the machined micro-channel on Aluminum 6061.

SEM images of the machined micro-channel at two different locations are shown in Figure 18a and b. Tool rotation direction is clockwise and more burr formation is observed on down milling side (left) as compared to up milling side (right). In mechanical micro-machining, burr formation is an inevitable phenomenon. A flexible abrasive pad is used to remove burrs from the micro-channel and the channel after deburring is shown in Figure 18c and d. It is observed that burr can be easily and effectively removed without damaging the dimensions of the micro-channel. After successfully milling 18 mm, the micro-channel is examined using a 3D optical profilometer for measuring shape and surface roughness. As shown in Figure 19, the channel shows a rectangular cross sectional profile and the average surface roughness along the full length of the channel is $R_a = 0.07$ µm. This proves that the tool is capable to be used as a micro-end mill tool for of micro-features.

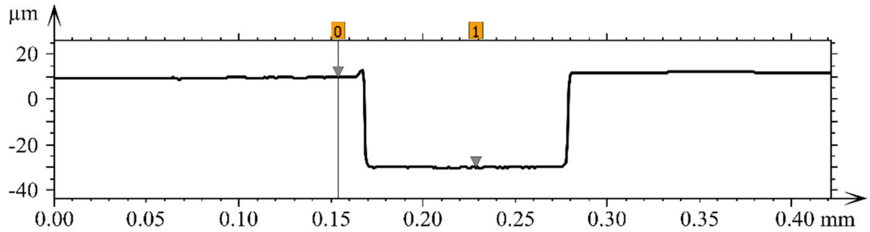

Parameters	0-1	Unit
Height difference	-39.901	µm

(a)

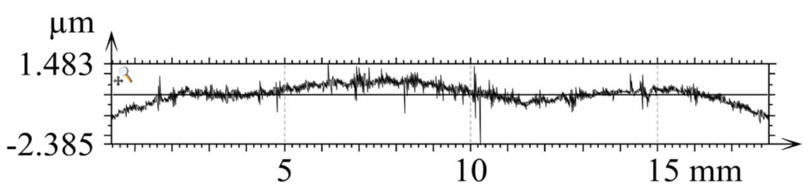

Parameters	Value	Unit			
Length	18.008	mm	Ra	0.070	µm

(b)

Figure 19. (a) Cross-sectional view along width and (b) surface roughness profile of the base of the machined micro-channel.

Figure 20 shows SEM images of the (a1) fabricated and (b1) commercial micro-end mill tool. Both the tools are used for machining of micro-channel on SS304L. Figure 20a2, b2 shows the micro-channel fabricated by both the tools. It is observed that channel fabricated by the present tool is smoother than the commercial tool. Cutting force readings are also shown in Figure 20a3, b3 and observed that no significant difference is observed. This ensures the feasibility of using the fabricated cutting tool for machining harder material like SS304L.

Conclusions

A parametric study is carried out to understand the effect of the selected process parameters and optimize them to fabricate a four edged end mill cutter. The following conclusions have been drawn from the study,

- Capacitance is the main factor that determines the dimensions of the cutting tool followed by voltage and spindle speed.
- It is found that voltage = 99 V, capacitance = 1 nF, spindle speed = 2573 rpm are the optimized level of the selected process parameters to

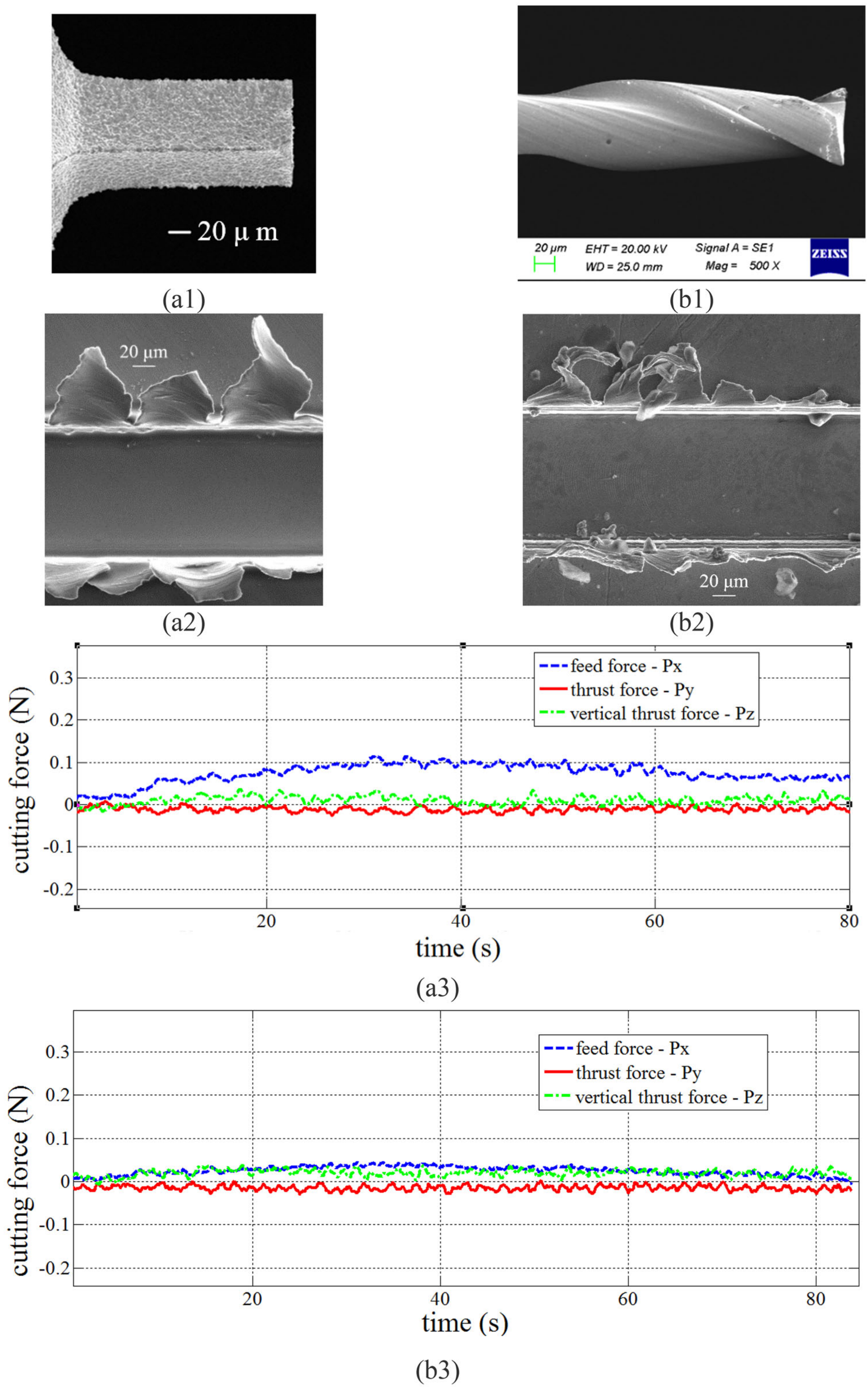

Figure 20. (a1, b1) SEM images, (a2, b2) micro-channel on SS304L and (a3, b3) cutting force readings of (a) the fabricated and (b) commercial micro-end mill tool.

get entrance dia. = 0.3225 mm, hole depth = 0.9567 mm, MRR = 0.0014 mm^3/min and surface roughness, Ra = 0.165 μm.

- The predicted overcut is used for tool path offsetting to increase the dimensional accuracy of fabricated micro-end mil tool.
- A tool of 100 μm diameter and 476 μm length is fabricated and it is used to machine a micro-channel of 18 mm length on Aluminum 6061.
- The fabricated channel has a rectangular cross sectional profile with a 110 μm width, 40 μm depth and a surface roughness of 70 nm.
- Machining performance of the fabricated tool is compared with the commercial end mill tool of 100 μm diameter. Smoother surface of micro-channel on SS304L is obtained by the fabricated end mill tool.

Disclosure statement

No potential conflict of interest was reported by the authors.

Funding

The authors acknowledge the funding support from the Institute under SGDRI grant, and Science and Engineering Research Board (SERB) under young scientist scheme (YSS).

ORCID

Ganesh Malayath https://orcid.org/0000-0003-3455-7512
Ajay M. Sidpara http://orcid.org/0000-0001-9998-3032

References

Adams, D.P.; Vasile, M.J.; Benavides, G.; Campbell, A.N. (2001). Micromilling of metal alloys with focused ion beam-fabricated tools. *Precision Engineering*, 25: 107–113. doi:10.1016/S0141-6359(00)00064-7

Aurich, J.C., Reichenbach, I.G., Schüler, G.M. 2012. Manufacture and application of ultra-small micro end mills. *CIRP Annals – Manufacturing Technology*, 61: 83–86. doi:10.1016/j.cirp.2012.03.012

Cheng, X.; Wang, Z.; Nakamoto, K.; Yamazaki, K. 2010. Design and development of PCD micro straight edge end mills for micro/nano machining of hard and brittle materials. *Journal of Mechanical Science and Technology*, 24: 2261–2268. doi:10.1007/s12206-010-0804-7

Chern, G.L.; Wu, Y.J.E.; Cheng, J.C.; Yao, J.C. 2007. Study on burr formation in micro-machining using micro-tools fabricated by micro-EDM. *Precision Engineering*, 31: 122–129. doi:10.1016/j.precisioneng.2006.04.001

Derringer, G.; Suich, R. 1980. Simultaneous optimization of several response variables. *Journal of Quality Technology*, 12: 214–219. doi:10.1080/00224065.1980.11980968

Ding, X.; Lim, G.C.; Cheng, C.K.; Butler, D.L.; Shaw, K.C.; Liu, K.; Fong, W.S. 2008. Fabrication of a micro-size diamond tool using a focused ion beam. *Journal of Micromechanics and Microengineering*, 18: 075017. doi:10.1088/0960-1317/18/7/075017

Egashira, K.; Hosono, S.; Takemoto, S.; Masao, Y. 2011. Fabrication and cutting performance of cemented tungsten carbide micro-cutting tools. *Precision Engineering*, 35: 547–553. doi:10.1016/j.precisioneng.2011.06.002

Ferreira, S.L.C.; Bruns, R.E.; Ferreira, H.S.; Matos, G.D.; David, J.M.; Brandão, G.C.; da Silva, E.G.P.; Portugal, L.A.; dos Reis, P.S.; Souza, A.S.; dos Santos, W.N.L. 2007. Box-Behnken design: An alternative for the optimization of analytical methods. *Analytica Chimica Acta*, 597: 179–186. doi:10.1016/j.aca.2007.07.011

Fleischer, J.; Deuchert, M.; Ruhs, C.; Kühlewein, C.; Halvadjiysky, G.; Schmidt, C. 2008. Design and manufacturing of micro milling tools. *Microsystem Technologies*, 14: 1771–1775. doi:10.1007/s00542-008-0652-x

Fonda, P.; Katahira, K.; Kobayashi, Y.; Yamazaki, K. 2012. WEDM condition parameter optimization for PCD microtool geometry fabrication process and quality improvement. *International Journal of Advanced Manufacturing Technology*, 63: 1011–1019. doi:10.1007/s00170-012-3977-7

Ganesh, M.; Sidpara, A.; Deb, S. 2017. Advanced Manufacturing Technologies 3–21. doi:10.1007/978-3-319-56099-1

Guckenberger, D.J.; de Groot, T.E.; Wan, A.M.D.; Beebe, D.J.; Young, E.W.K. 2015. Micromilling: a method for ultra-rapid prototyping of plastic microfluidic devices. *Lab on a Chip*, 15: 2364–2378. doi:10.1039/C5LC00234F

Habib, S.; Okada, A. 2016. Influence of electrical discharge machining parameters on cutting parameters of carbon fiber-reinforced plastic. *Machining Science and Technology*, 20: 99–114. doi:10.1080/10910344.2015.1133914

Han, F.; Yamada, Y.; Kawakami, T.; Kunieda, M. 2006. Experimental attempts of submicrometer order size machining using micro-EDM. *Precision Engineering*, 30: 123–131. doi:10.1016/j.precisioneng.2005.06.005

Jabbaripour, B.; Sadeghi, M.H.; Faridvand, S.; Shabgard, M.R. 2012. Investigating the effects of EDM parameters on surface integrity, MRR and TWR in machining of Ti-6Al-4V. *Machining Science and Technology*, 16: 419–444. doi:10.1080/10910344.2012.698971

Jafferson, J.M.; Hariharan, P.; Ram Kumar, J. 2016. Effect of non-electrical parameters in μED milling: an experimental investigation. *International Journal of Advanced Manufacturing Technology*, 85: 2037–2047. doi:10.1007/s00170-015-7933-1

Jahan, M.P.; Wong, Y.S.; Rahman, M. 2012. Experimental investigations into the influence of major operating parameters during micro-electro discharge drilling of cemented carbide. *Machining Science and Technology*, 16: 131–156. doi:10.1080/10910344.2012.648575

Jahan, M.P.; Wong, Y.S.; Rahman, M. 2009. A study on the quality micro-hole machining of tungsten carbide by micro-EDM process using transistor and RC-type pulse generator. *Journal of. Materials Processing Technology*, 209: 1706–1716. doi:10.1016/j.jmatprotec.2008.04.029

Karthikeyan, G.; Ramkumar, J.; Dhamodaran, S. 2014. Block EDG: Issues and applicability in multiple pass μED-milling. *Machining Science and Technology*, 18: 120–136. doi:10.1080/10910344.2014.863650

Kawasaki, K.; Nishiguchi, T.; Miyajima, T.; Higuchi, S.; Fukazawa, K. 2013. Precision cutting of molding die using square end mill. *Machining Science and Technology*, 17: 93–109. doi:10.1080/10910344.2012.747907

Koo, J.Y.; Kim, J.S.; Kim, P.H. 2014. Machining characteristics of micro-flow channels in micro-milling process. *Machining Science and Technology*, 18: 509–521. doi:10.1080/10910344.2014.955360

Lee, H.W.; Choi, H.Z.; Lee, S.W.; Choi, J.Y.; Jeong, H.D. 2002. A study on the micro tool fabrication using electrolytic in-process dressing. *Journal of the Korean Society for Precision Engineering*, 19: 171–178.

Montgomery, D.C. 2008. Design and Analysis of Experiments, Design and Analysis of Experiments. John Wiley & Sons, New York.

Morgan, C.J.; Vallance, R.R.; Marsh, E.R. 2004. Micro machining glass with poly crystalline diamond tools shaped by micro electro discharge machining. *Journal of Micromechanics and Microengineering*, 14: 1687–1692. doi:10.1088/0960-1317/14/12/013

Nakamoto, K.; Katahira, K.; Ohmori, H.; Yamazaki, K.; Aoyama, T. 2012. A study on the quality of micro-machined surfaces on tungsten carbide generated by PCD micro end-milling. *CIRP Annals – Manufacturing Technology*, 61: 567–570. doi:10.1016/j.cirp.2012.03.112

Ohmori, H.; Katahira, K.; Naruse, T.; Uehara, Y.; Nakao, A.; Mizutani, M. 2007. Microscopic grinding effects on fabrication of ultra-fine micro tools. *CIRP Annals – Manufacturing Technology*, 56: 569–572. doi:10.1016/j.cirp.2007.05.136

Onikura, H.; Ohnishi, O.; Take, Y. 2000. Fabrication of micro carbide tools by ultrasonic vibration grinding. *CIRP Annals – Manufacturing Technology*, 49: 257–260. doi:10.1016/S0007-8506(07)62941-2

Perveen, A.; San, W.Y.; Rahman, M. 2012. Fabrication of different geometry cutting tools and their effect on the vertical micro-grinding of BK7 glass. *International Journal of Advanced Manufacturing Technology*, 61: 101–115. doi:10.1007/s00170-011-3688-5

Picard, Y.N.; Adams, D.P.; Vasile, M.J.; Ritchey, M.B. 2003. Focused ion beam-shaped microtools for ultra-precision machining of cylindrical components. *Precision Engineering*, 27: 59–69. doi:10.1016/S0141-6359(02)00188-5

Sharma, R.K.; Singh, J. 2016. Determination of multi-performance characteristics for powder mixed electric discharge machining of tungsten carbide alloy. Proceedings of the Institution of Mechanical Engineers Part B Journal of Engineering Manufacture, 230: 303–312. doi:10.1177/0954405414554017

Suzuki, H.; Okada, M.; Fujii, K.; Matsui, S.; Yamagata, Y. 2013. Development of micro milling tool made of single crystalline diamond for ceramic cutting. *CIRP Annals – Manufacturing Technology*, 62: 59–62. doi:10.1016/j.cirp.2013.03.096

Tak, H.S.; Ha, C.S.; Kim, D.H.; Lee, H.J.; Lee, H.J.; Kang, M.C. 2009. Comparative study on discharge conditions in micro-hole electrical discharge machining of tungsten carbide (WC-Co) material. *Transactions of Nonferrous Metals Society of China (English Ed)*, 19: s114–s118. doi:10.1016/S1003-6326(10)60257-9

Uhlmann, E.; Oberschmidt, D.; Löwenstein, A.; Kuche, Y. 2016. Influence of cutting edge preparation on the performance of micro milling tools. *Procedia CIRP*, 46: 214–217. doi:10.1016/j.procir.2016.03.204

Wang, A.C.; Yan, B.H.; Tang, Y.X.; Huang, F.Y. 2005. The feasibility study on a fabricated micro slit die using micro EDM. *International Journal of Advanced Manufacturing Technology*, 25: 10–16. doi:10.1007/s00170-003-1831-7

Wang, C.; Gong, Y.; Cheng, J.; Wen, X.; Zhou, Y. 2016. Fabrication and evaluation of micromill-grinding tools by electroplating CBN. *International Journal of Advanced Manufacturing Technology*, 87: 3513–3526. doi:10.1007/s00170-016-8730-1

Yan, B.H.; Huang, F.Y.; Chow, H.M.; Tsai, J.Y. 1999. Micro-hole machining of carbide by electric discharge machining. *Journal of Materials Processing Technology*, 87: 139–145. doi:10.1016/S0924-0136(98)00345-8

Zhan, Z.; He, N.; Li, L.; Shrestha, R.; Liu, J.; Wang, S. 2015. Precision milling of tungsten carbide with micro PCD milling tool. *International Journal of Advanced Manufacturing Technology*, 77: 2095–2103. doi:10.1007/s00170-014-6632-7

Zhang, Z.; Peng, H.; Yan, J. 2013. Micro-cutting characteristics of EDM fabricated high-precision polycrystalline diamond tools. *International Journal of Machine Tools and Manufacture*, 65: 99–106. doi:10.1016/j.ijmachtools.2012.10.007